

# CaLIPSO: An Novel Detector Concept for PET Imaging

D. Yvon, J.-Ph. Renault, G. Tauzin, P. Verrecchia, C. Flouzat, S. Sharyy, E. Ramos, J.-P. Bard, Y. Bulbul, J.-P. Mols, P. Starzynski, D. Desforge, A. Marcel, J.-M. Reymond, S. Jan, C. Comtat, and R. Trébossen

**Abstract**—The CaLIPSO project focuses on the development of an innovative energetic-photon detector. The detector uses a “heavy” organometallic liquid: the TriMethyl Bismuth (TMBi), 82% by weight of Bismuth. TMBi efficiently converts through the photo-electric effect photons of energies below 1 MeV. The ionisation signal and light produced in the liquid are both detected. Beyond the measurement of gamma photon energies, this detector will allow locating photon interactions in the detector in three dimensions down to  $1 \text{ mm}^3$  and a sub nanosecond timing accuracy. All these desirable properties can be obtained simultaneously with liquid TMBi detector.

**Index Terms**—Biomedical imaging, calorimetry, gamma ray detectors, position sensitive particule detectors, positron emission tomography.

## I. INTRODUCTION

PET imaging is used for diagnosis, clinical research and in vivo small animal research to study molecular processes associated with cancer, neurological and neurodegenerative diseases, psychiatry and cardiology. Since the early 1990 when PET was recognized as a powerful diagnosis tool, major technological advances have been made mainly in the five following directions: 1) sensitivity improvement, 2) spatial resolution gain, 3) uniformity of the spatial resolution across the field of view, 4) corrections for the main effects degrading the quantification, and 5) reconstruction algorithms so as to improve the signal to noise ratio and the spatial resolution of images.

These efforts have translated to the advent of dedicated small animal imaging devices, TOF PET and high spatial resolution whole body PET systems. In addition to these improvements, an

Manuscript received June 10, 2013; revised August 21, 2013; accepted November 06, 2013. Date of publication January 09, 2014; date of current version February 06, 2014. This work was supported in part by the Neuropole de Recherche Francilien (NeRF), Ile de France, under the Grant no. RPH10014DDA.

D. Yvon, G. Tauzin, P. Verrecchia, C. Flouzat, S. Sharyy, E. Ramos, J.-P. Bard, Y. Bulbul, J.-P. Mols, P. Starzynski, D. Desforjes, A. Marcel, and J.-M. Reymond are with CEA Saclay, Institut de Recherche sur les lois Fondamentales de l'Univers, Bat. 141, F-91191 Gif sur Yvette Cedex (e-mail: dominique.yvon@cea.fr).

J.-Ph. Renault is with CEA Saclay, IRAMIS/SIS2M and UMR 3299 CNRS, Bat 546, F-91191 Gif sur Yvette Cedex.

S. Jan, C. Comtat and R. Trébossen are with the CEA-Service Hospitalier Frédéric Joliot, 4 place du Général Leclerc, F-91401 Orsay Cedex.

Color versions of one or more of the figures in this paper are available online at <http://ieeexplore.ieee.org>.

Digital Object Identifier 10.1109/TNS.2013.2291971

TABLE I  
MAIN RECENT SCINTILLATOR CRYSTALS PROPERTIES

		LSO	LYSO	LaBr <sub>3</sub>
Density	$\text{g.cm}^{-3}$	7.4	7.1	5.3
RapPE	%	30	30	15
Att. Coeff.	$\text{cm}^{-1}$	0.87	0.86	0.47
Light Yield	$\text{MeV}^{-1}$	30000	32 000	63 000
Dec. time	ns	40	41	25
Hydroscopic		No	No	Yes

effort toward multimodalities imaging systems including PET is ongoing.

Most PET detectors use Lutetium-based crystals such as LSO and/or LYSO scintillator crystals [1], [2], [3]. Recently LaBr<sub>3</sub> scintillation crystal has been proposed as an alternative to lutetium based crystals. Table I summarizes the main properties of those crystals. Those detectors have opened the way to advanced performance PET systems in the early 2000s. Roger Lecomte has detailed in reference [3] the performance requirements for clinical PET and described the detection technologies and their assembly into systems.

The state of the art commercially available PET systems exhibit nearly 10% efficiency. This moderate value mainly results from the limited solid angle coverage. Indeed, most of PET systems are cylindrical and their axial extension is limited to 20 to 25 cm at best.

Furthermore 511 keV-photons that enter an LSO scintillating crystal have 70% chance to Compton scatter. If the crystal is large enough, double interactions are likely to occur and ensure the full conversion of photon energy. However these events introduce an ambiguity in the interaction positioning and will also impact the spatial resolution. As a consequence a detector material with a high **photo fraction** is valuable for PET imaging [2] as it will enable the development of a compact system with optimal spatial resolution and preserved detection efficiency.

Improvement of the spatial resolution and its uniformity across the Field of View (FOV) were proposed with the measurement of the photon depth of interaction and the 3D positioning of the photon interactions in the detectors [2], [3]. However, in most of commercially available systems, intrinsic spatial resolution is limited by detector crystal size, photon noncolinearity and to a less extent to the positron range.

A *detector time resolution* of a few 100 ps allows localizing the position of the positron annihilation with several-cm accuracy along the Line Of Response. This time resolution efficiently reduces the random background impact on the image

TABLE II  
MAIN PARAMETERS OF IONISATION DETECTORS, INCLUDING TECHNOLOGIES TAKING ADVANTAGES OF SIMULTANEOUS DETECTION OF LIGHT

	Dens.	Att. Coeff	Rap. PE	Light Yield	Decay Time	Ion. Yield	Elec. Mobility	Cryo. needed
	$g.cm^{-3}$	$cm^{-1}$	%	$MeV^{-1}$	$ns$	$keV^{-1}$	$cm^2/\mu s/kV$	
CdZnTe	6.0	0.52	16	-	-	200	1.35	No
Xenon	2.95	0.28	24	1.9-4.5e5	2.2 - 27 and 45	64	0.18	Yes
TMSi	0.648	0.063	0.04	54-84	~0.1	10	0.08	No
TMBi	2.3	0.40	47	44 - 93	~0.1	TBM*	TBM*	No

TBM\* means to be measured. To date only charge mobility in TMBi has been demonstrated. But many similar liquid have been measured in the past with electronic properties close to TetraMethylSilane (TMSi).

noise [5]. Among the latest proposed scintillation crystals, the  $LaBr_3$  has the best timing properties. The coincidence resolving time may reach 100 ps on small samples [8] and a 375 ps time resolution was measured on a prototype TOF PET scanner [5]. The drawback is the reduced crystal density, reduced photo-fraction and crystal hydroscopy.

To avoid these problems with scintillation crystals one can use ionization detectors. Table II summarizes the main properties of the three materials proposed for PET.

High atomic number semiconductor materials, CZT, and CdTe have the assets of excellent energy resolution, compactness and take advantage of the electronic micro-structuration technologies. Both semiconductor technologies have been or are being studied for PET imaging systems [9], [10]. Indeed CdTe semiconductor technology allowed building a very high resolution small animal PET scanner [11]. The main drawbacks of semiconductor for PET imaging results from their low speed, their moderate stopping power, low photo-fraction and their cost.

Resistive Plate Chamber technology (RPC) uses a multilayer gaseous particle detector. 511 keV photon interactions mainly happen in detector electrodes. The electrons produced in these interactions can escape from the electrodes and trigger cascades in the neighboring gas-filled gap. These detectors show good timing properties (adequate for TOF measurement), accurate interaction positioning, and very low cost. Their main disadvantages result from the high attenuation length, the low photoelectric efficiency and low energy resolution [12]. But because of the low detector cost, authors propose building a whole body, single bed TOF RPC PET [13]: the large solid angle compensates for the modest detector efficiency.

A liquid Xenon detector is a double detector: both scintillation light and ionisation signals are detected. The technology of liquid “noble gas” detectors is now mature and a review of the technological options and applications is exposed in reference [14]. Scintillation signal has light yield, and includes a component of very fast decay time: subnanosecond timing resolution has been demonstrated [15]. Because electron diffusion is very small [16], liquid xenon drift chamber showed a submillimeter spatial resolution in 3 dimensions [17], [18]. In addition, simultaneous detection of scintillation and ionization lead to energy resolution of 10% FWHM on 511 keV gamma with a prototype TEP module [19], and of 6.2% on small optimized devices [20].

Thanks to the very good spatial and energy resolution, several groups are working on Compton telescope detector that would allow recovering some of the Compton interaction occurring into

the detector. Reference [21] proposes to take advantage of  $^{44}Sc$  radionuclide properties to implement a new nuclear imaging technique allowing the measurement of 3D emitter location. In summary, liquid xenon devices are versatile high-technology detectors. Their use for medical imaging application is limited by the low stopping power, moderate photo-fraction, and the need of a recycling and cryogenic system for maintaining a low temperature operation.

This paper presents a new detector concept, CaLIPSO, and compares its potential with the characteristics of presently used detectors in PET systems. CaLIPSO is the acronym for “Calorimetre Liquide Ionisation, Position Scintillation Organometallique”. This detector project takes advantage of the very high atomic number of bismuth and of modern instrumentation technologies to target improved PET performance.

In Chapter II, we detail the CaLIPSO detector material choice, the detector basics and the bibliography supporting the design options. We show the expected CaLIPSO detector performance.

In Chapter III, we report preliminary tests on small devices that show the potential of TMBi material for 511 keV gamma detection.

Paragraph IV discusses the technological challenges required for operating a CaLIPSO detector and draw tracks for future PET system design.

## II. CALIPSO DETECTOR

Liquefied “noble-gas” detectors have been the guideline for CaLIPSO project. If they contain heavy elements, they would have all the detector properties required for PET. In that purpose, “sandwich” detectors have been proposed, stacking heavy metal sheets immersed in liquefied noble-gas detectors. But energy loss in metal sheet would not contribute to detected signal, leading to a strongly degraded energy resolution incompatible with Compton rejection. Thus heavy metal must be incorporated to the detection medium *at the molecular level*.

However, liquefied noble-gas are bad solvent (aprotic, apolar), so loading a liquefied noble gas with a heavy metal based molecule would produce a medium with low heavy-metal mass fraction.

Molecules have an electronic structure similar to noble gas. Charge drift has been demonstrated in such ultrapure liquids in the past, (TMSi, TMGe, TMSn, TMP [22], [23]).

We selected organometallic complexes, since they have the following specifications:

- chemical stability;

- high density;
- high effective atomic number;
- liquid at room temperature;
- insulator;
- involving no electronegative compound either as primary components or unavoidable contaminants (purifiable).

Such complexes possess almost nonpolarized metal carbon bonds that decrease intermolecular interaction in the condensed state. As a consequence, organometallic can have relatively low melting and boiling points compared to complexes with more polar ligands (like those containing oxygen and nitrogen). Furthermore, their phase transition temperature can be tuned by changing the size of the ligands. They have also low oxidation numbers that decrease their tendency to trap electrons.

Amongst possible ligands, we focused on carbonyl (CO) or on alkyl ( $C_nH_{2n+1}$ ). However, carbonyl compounds are better described for low Z metals and alkyl for high Z ones. Some high Z metal alkyl compounds have even been produced on an industrial scale. ( $PbEt_4$  as an additive for gasoline)

Among Mercury, Pb and Bi compounds, we selected Bi because of its lower number of ligands (3 compared to 4) which allows a higher electronic density in the liquid phase and low toxicity (compared to Hg).  $Bi(CH_3)_3$  is a commercial compound used in the electronic industry that can be obtained with a high initial purity (> 99,99%) at moderate cost.

Furthermore, even though alkyl organometallics are less stable than pure organic compounds,  $Bi(CH_3)_3$  is self healable with respect to the application considered here, as its decomposition produces only gas ( $C_2H_6$ ) and solid (Bi) that are not expected to interfere with the detection process.  $Bi(CH_3)_3$  has one drawback: he is a pyrophoric liquid: it has to be manipulated under anoxic conditions and discarded appropriately. Since the liquid has to be ultra-purified and kept clean from all electronegative impurities, including oxygen, this inconvenient is handled by using ultra-vacuum technologies in handling and storing the detection material.

### A. Detector Basics

When the project started, TMBi had never been used in particle detector. But the WALIC project [24Aubert1990] has studied charge drift in several ultra-pure organometallic liquids TetraMethylSilane (TMSi), TetraMethylGermane, TetraMethylTin (TMSn), TetraMethyl Pentane (TMP) etc.... TMSi is a well known dielectric used since the 90s as sensitive medium in ionization chambers [25], [26].

We used the main design of liquid Xenon detectors except that xenon is replaced with a heavy organometallic liquid to efficiently convert MeV photons. TMBi (Trimethyl Bismuth [27], [28]) contains 82% by weight of bismuth  $^{209}_{83}Bi$ . TMBi is a stable limpid chemical.

When a 511 keV photon enters the detector (Fig. 1), it is likely to interact through photo-electric effect with a bismuth atom. A K-shell electron (so called primary electron) is ejected with 420 keV kinetic energy. This electron is relativistic in TMBi. It produces light through the Cerenkov effect and ionization along

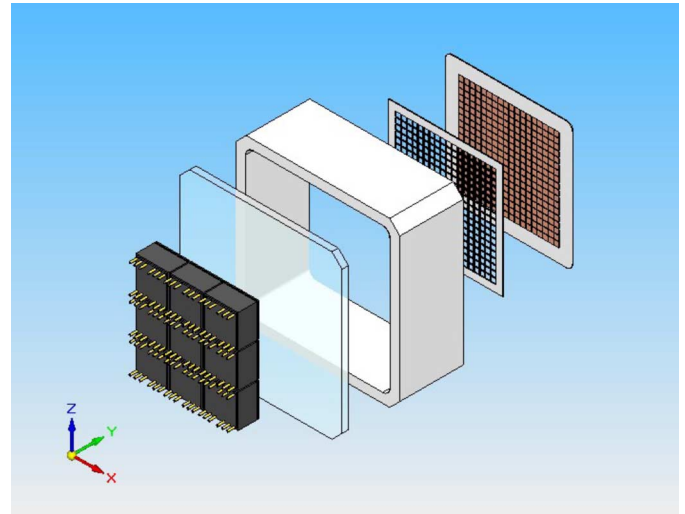


Fig. 1. Principle of the CaLIPSO detector. The box volume is filled with liquid TMBi. Photomultipliers (black cubes) look at the liquid through a glass window, and detect Cerenkov photons produced in the liquid. Pixellated charge detector (brown) collects ionisation signals behind a Frisch grid (black). The first prototype should have an active surface of  $10 \times 10 \text{ cm}^2$  and a thickness of 5 cm. Because of TMBi reactivity, and cleaning requirement, we will use alumina ceramics, glass and stainless steel, whenever possible. (see text for more details).

it path. We will detect both the charges and the light produced by the primary electron.

The detector is an ionisation chamber filled with ultra-pure TMBi: the electrons freed by the ionising radiation drift in a strong electric field, until they go through a Frisch grid [29], 1 mm before reaching a *pixelated* electric circuit. Assuming TMBi has similar properties as TMSi, TMGe, TMP [22], we expect the production  $\sim 4500$  free electrons.

Charge detection will be used for energy measurement and interaction positioning in the charge collection plane. We will use the IDEF-X 2E charge amplifier technology to readout the charge detector pixels. This is a low noise ASICS device developed in our lab [30][31]. IDEF-X ASICS have been used to readout detectors with  $0.34 \text{ mm}^2$  pixels [32].

Transport properties of electrons in TMSi have never been studied in details. Reference [33] quote the mean energy of electrons in TMSi versus electric field, but not the transverse energy, needed for computing charge transverse diffusion during drift. The transverse energy is known to be of the same order as mean electron energy in liquids, but significantly larger when the drift electric field exceed few kV/cm [16]. From [33] we get a mean energy value for a free electron in TMSi of 0.04 eV. Assuming a factor 10 excess for the transverse energy at drift field value of 10 kV/cm, we compute a transverse size for the ionization cloud of  $210 \mu\text{m} \cdot L^{-1/2}$  (FWHM), L (expressed in cm) being the distance over which charge drifts in the ionization chamber. The detector position accuracy is thus expected to be dominated by the size of the detector collection pads.

With IDEF-X chips we compute a readout noise lower than 200 electrons FWHM and a timing accuracy of 100 ns. Assuming 4500 free-electrons production on a 511 keV photo-electric conversion, the intrinsic charge production width is expected to be 158 electrons FWHM, slightly less than readout electronic noise. If charge trapping were negligible, we would



Fig. 2. Optical timing cell, outside of its housing. Two fast photomultipliers are mounted on the glass windows looking at the TMBi volume.

expect an energy resolution of 5.7%. For this work we hope to obtain a resolution of 10%. Reference [34] quotes an energy resolution of 12.7% (FWHM) on 976 keV electrons, dominated by readout noise.

Cerenkov light production yield is low, (we measured from 10 to 18 photoelectrons/MeV using XP1911 photomultipliers [35]), but happens in a very short time. We will use the detection of the first photoelectron to trigger the detector and date the particle interaction. Monte Carlo simulations foresee sub-ns timing accuracy. Careful light collection will have to be enforced to ensure efficient triggering of the detector and optimize timing resolution.

The combination of the two detectors will give us access to the electrons drift time in liquid TMBi, from which the interaction location within the thickness of the detector can be deduced. Electron drift velocity in TMSi has been measured  $1 \text{ cm}/\mu\text{s}$  at  $10 \text{ kV/cm}$  drift field [22].  $0.1 \mu\text{s}$  time resolution on charge detection should allow  $1 \text{ mm}$  positioning accuracy for interaction in the detector thickness.

### III. TESTS ON SMALL DEVICES—METHODS AND RESULTS

Measurements methods and results of TMBi *optical properties* for particle detection are given in reference [35].

In the following, we show test measurements on small samples and summarize results that support the proposed detector idea.

#### A. First TMBi Timing Performances Test

TMBi is a transparent liquid. We built a small size test cell, in order to demonstrate the timing potential of TMBi based detector. The timing cell shown at Fig. 2, enclosed a  $8 \text{ mm}$  long volume of TMBi observed by two fast Hamamatsu R9800U Photomultipliers. When exposed to a  $^{22}\text{Na}$  radioactive source, coincident events pulses shapes were recorded and analysed [35].

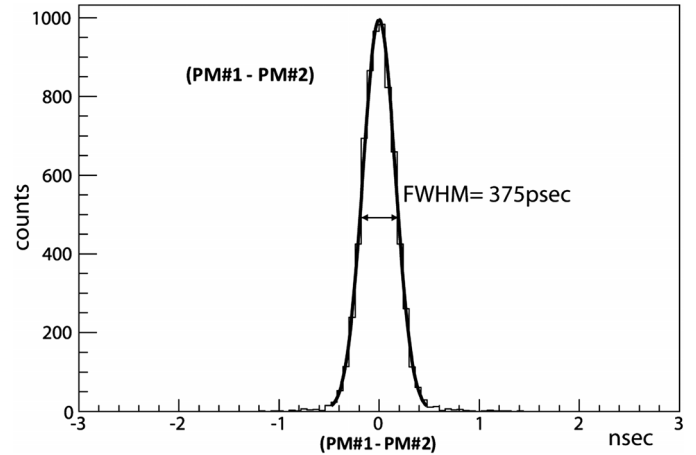


Fig. 3. Histogram of the time difference as measured by two PMTs looking at 511 keV interactions in the optical timing cell.

Fig. 3 plots the histogram of the time difference measured on PMTs signals. We measured a width of 375 ps FWHM, with un-optimised electronics. Main identified time width contributions are PMTs Time Transit Spread (280 ps FWHM), random optical path difference (52 ps), and data acquisition jitter (40 ps). The remaining width contribution amounts to 237 ps (FWHM) and is dominated by noise-induced jitter on pulse shapes. The contribution of intrinsic Cerenkov light production to this width is negligible.

#### B. Electron Mobility and Preliminary Free Ion Yield in Liquid TMBi

Detecting 511 keV single event in TMBi requires to achieve ultra-purification of the liquid. For a convenient use of the foreseen detector, the free electron lifetime in TMBi should be larger than  $50 \mu\text{s}$ . In liquid TMSi such a lifetime corresponds to a contamination level of 0.1 ppb equivalent oxygen [26]. We did not achieve this purity yet. But before that, we wanted to demonstrate the hypothesis of electron mobility in TMBi. Following, we report a measurement of the field dependence of the free ion yield for TMBi.

We built two identical ionization chambers (Fig. 4), one for liquid TMBi and one for TMSi. These cells were mounted from a stainless steel vessel of about  $20 \text{ ml}$  volume, assembled using standard high vacuum techniques and connected to their dedicated gas handling and vacuum system. Liquids were transferred into their dedicated chamber using cryogenics transfer. One cell is filled with TMSi (from MERCK grade 99.97%) the other cell with TMBi (JSC Alkyl 99.999%). The liquids were used without any further purification.

In both Cells, ionization current is measured (using KEITHLEY 6517 model A, Amp-meter), when the radiation field of a  $^{60}\text{Co}$  source ( $1.7 \text{ Mbq}$ ) covers the whole chamber.

For TMSi and TMBi dielectric liquids, the ionization current increases linearly with electric field strength above  $0.050 \text{ MV/m}$  as expected in most ionization models. Reference [38] described this behavior, quantified relations for liquid iso-octane and TMSi and [39] made a comparison with the Onsager model. This is the method we use in this article for both TMSi and TMBi: assuming the ionization current is proportional to the number of

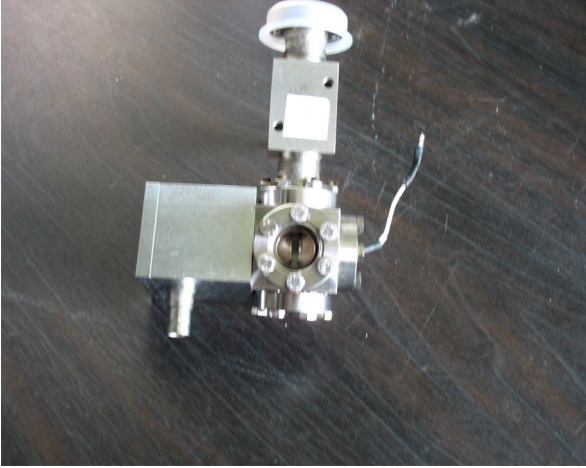


Fig. 4. Gfi Cell with HV connector box, readout cable and valve. Behind the porthole we see the cathode and the anode (stainless steel 1.55 cm diameter, 0.5 mm thick, 2 mm gap) soldered to a ceramic ( $Al_2O_3$ ) support.

electron-ion pairs released in the liquid per second, we deduce the free ion yields. The energy deposit in each liquid is computed from Monte Carlo.

Free ion yield (the so called Gfi), is quantified as the number of ion pairs detected per 100 eV energy absorbed. The ratio  $G_{fi}^{TMBi}(E)$  to  $G_{fi}^{TMSi}(E)$  is plotted in Fig. 5. This preliminary result indicates that both liquids have similar ionization yields:

- 1) The experimental relationship between free ion yield ratio and electric field is found linear in the low field strength region as expected by the Onsager's theory
- 2) Extrapolating the linear fit to zero fields, we found that the free ion yield of TMBi is  $(78.8 \pm 1.7)\%$  of the free ion yield of the TMSi at zero electric field.
- 3) Slopes of  $G_{fi}(E)$  in the low field region are almost identical for both liquids.

#### IV. DISCUSSION

##### A. First Results

The width of the coincidence-time distribution is 375 ps. While this is adequate for PET imagers, it is significantly worse than the best performance of test devices using Cherenkov light or LaBr3 scintillators [8], [42], [43]. The main reason is that we did not use Micro-Channel Plate photomultipliers for photon detection and that we were mainly detecting single photoelectrons. Achieving less than 100 ps FWHM timing accuracy and a adequate detection efficiency should be possible but will require [43] improving light collection efficiency (stainless steel was measured to be a poor light-guide reflector), and optical coupling between TMBi and the PMT photocathode. This first measurement should be considered as a demonstration of principle of the CaLIPSO technology, for Time-Of-Flight PET.

Several room temperature liquids have been studied as media for ionization chambers. Some of them have high electron mobility as well as a large  $G_{fi}$ . Such characteristics have been found for neopentane [36] and TMSi [37] and for others liquids containing germanium and tin atom [22].

This  $G_{fi}$  measurement on TMBi is a preliminary result: our measurements to date are mainly sensitive to the purity level

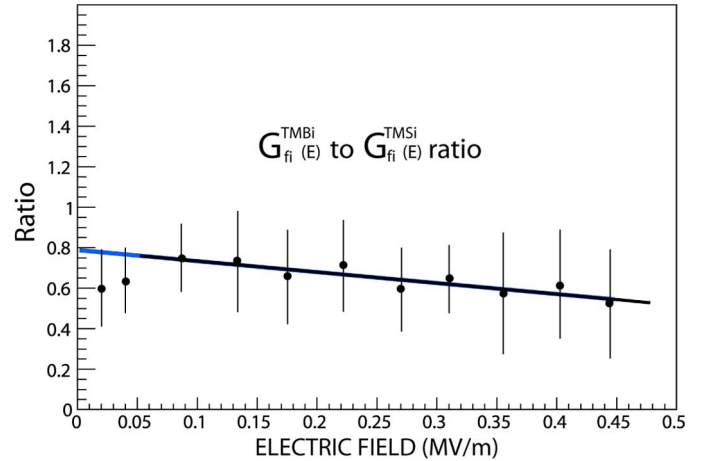


Fig. 5.  $G_{fi}^{TMBi}(E)$  to  $G_{fi}^{TMSi}(E)$  ratio as a function of applied electric field. A linear fit is performed in the low field strength region [0.6, 4.6 kV/cm].

of both liquids, thus to the *collection efficiency* of the electrons released in the ionization process. Nevertheless these first measurements of the free ion yields demonstrated electron mobility in liquid TMBi. And we have indication that this dielectric liquid behaves similarly as the other liquid composed of methyl ( $CH_3$ ) groups around the central atom.

##### B. Technological Challenges

We have identified three remaining technological challenges for the CaLIPSO detector:

- *The TMBi must be ultra-purified*, to allow free electron drift, and the measurement of gamma energies. We organised all the preparatory and detector-mounting work, at the IrFU/SEDI clean rooms. The materials, from which the detector is made, shall be carefully chosen and cleaned [26], [40].
- *The low light production efficiency* will require careful optimisation of the optical couplings, and careful selection of the photodetectors, in order to ensure efficient triggering of 511 keV photons. This issue is currently addressed by tests on our optical demonstrator devices.
- *The electronic readout density*. Integrating an electronic density of 1 preamplifier per  $mm^2$  is a challenge. But this has already been achieved in the laboratory, with low noise performances using 3D electronics [32] in the context of a spaceborne experiment.

##### C. PET Motivations for CaLIPSO

The proposed CaLIPSO detector is at its first stage of development. We feel that the CaLIPSO has a great potential in the field of PET-scan instrumentation.

The main advantages of xenon detectors are kept. CaLIPSO technology, through the double detection of the charge signal and the production of optical photons, should allow interactions positioning in the liquid with an accuracy of  $1 mm^3$ , and a sub-nanosecond time resolution. The expected energy resolution on 511 keV photons is adequate for TEP imaging: 10% FWHM or better. Furthermore, CaLIPSO detector has assets when compared to liquid xenon detectors:



- Because of its large mass fraction of Bismuth, liquid TMBi has excellent photofraction values. In the proposed configuration (a 5 cm thick detector), 85% of the 511 keV photons would interact in the TMBi, within of those, 47% would convert through the photoelectric effect.
- Liquid TMBi has improved stopping power, and the detector does not need cryogenic to run: this allows to build more compact detectors.

Overall, calculated performances match very well the specifications of a detector optimised for PET scan imaging. We notice that these desirable properties can be obtained simultaneously with liquid TMBi detectors: improved photofraction coupled to interaction position reconstruction should allow designing high spatial resolution, efficient PET-scan imagers, on large volumes. In addition, the foreseen energy resolution should allow the efficient rejection of Compton diffusions in organs.

TMBi is a very demanding detector medium at the development stage: light signal is minimal, ionisation signal requires ultra-purification of liquid, beyond what is required for xenon detectors. But we are convinced that modern technologies will allow us to overcome these issues.

## V. CONCLUSION AND PERSPECTIVES

The CaLIPSO detector using liquid TMBi has the potential to become a breakthrough in PET-scan imager technology. Calculated performances are promising. This detector is very demanding on hardware performances. Lab tests are at the first stages of development.

CaLIPSO detector has been designed to fulfill the specification list of an enhanced PET-scan imager, but it is likely that many demanding use of a positron detector would probably benefit from CaLIPSO technology.

Our developpement plan includes building and testing an optical demonstration detector and a charge demonstration detector separately. Once debugged and optimized the two technologies will be assembled.

## ACKNOWLEDGMENT

The authors wish to thank J. Rich for carefully reading the proofs and the Referees for stimulating comments.

## REFERENCES

- [1] R. Trébossen, "Recent innovations in the detection systems of Positron Emission Tomography," *Med. Nucléaire*, vol. 31, pp. 126–131, 2007.
- [2] T. K. Lewellen, "Recent developments in PET detector technology," *Phys. Med. Biol.*, vol. 53, pp. R287–R317, 2008.
- [3] R. Lecomte, "Novel detector technology for clinical PET," *Eur. J. Nucl. Med. Mol. Imag.*, vol. 36, pp. S69–S85, 2009.
- [4] Levine and Hoffman, *Phys. Med. Biol.*, vol. 44, p. 781, 1999.
- [5] M. E. Daube-Witherspoon, S. Surti, A. Perkins, C. C. M. Kyba, R. Wiener, M. E. Werner, R. Kulp, and J. S. Karp, "The imaging performance of a LaBr3-based PETScanner," *Phys. Med. Biol.*, vol. 55, pp. 45–64, 2010.
- [6] S. Surti, A. Kuhn, M. E. Werner, A. E. Perkins, J. Kolthammer, and J. S. Karp, *J. Nucl. Med.*, vol. 48, pp. 471–480, 2007.
- [7] Moses and Derenzo, "Timing resolution of LSO detector 300-500 ps," *IEEE-TNS* 1999.
- [8] D. R. Schaart, S. Seifert, R. Vinke, H. T. van Dam, P. Dendooven, H. L. Ohner, and F. J. Beekman, "LaBr3:Ce and SiPMs for time-of-flight PET: Achieving 100 ps coincidence resolving time," *Phys. Med. Biol.*, vol. 55, pp. N179–N189, 2010.

- [9] G. Montémont, C. Comtat, P. Descourt, S. Jan, M. Leabad, S. Maître-jean, and F. Mathy *et al.*, "TOPASE-MED: Rethinking PET imaging with semiconductor detectors," *IRBM*, vol. 31, p. 73, 2010.
- [10] Y. Yin, S. Komarov, H. Wu, T. Yong Song, Q. Li, and A. Garson, III *et al.*, "Characterization of highly pixelated CZT detectors for sub-millimeter PET imaging," in *Proc. IEEE NSS Conf. Rec.*, 2009, p. 2411.
- [11] K. Ishii, Y. Kikuchia, S. Matsuyama, Y. Kanaia, K. Kotanib, and T. Ito *et al.*, "First achievement of less than 1 mm FWHM resolution in practical semiconductor animal PET scanner," *NIMA*, vol. 576, p. 435, 2007.
- [12] A. Blanco, N. Carolino, C. M. B. A. Correia, L. Fazeiro, N. C. Ferreira, and M. F. Ferreira Marques *et al.*, "RPC-PET: A new very high resolution PET technology," *IEEE Trans. Nucl. S.*, vol. 53, p. 2498, 2006.
- [13] P. Crespo, J. Reis, M. Couceiro, A. Blanco, N. C. Ferreira, and R. Ferreira Marques *et al.*, "Whole-Body single-bed time-of-flight RPC-PET: Simulation of axial and planar sensitivities with NEMA and anthropomorphic phantoms," *IEEE TNS*, vol. 59, p. 520, 2012.
- [14] E. Aprile and T. Doke, "Liquid xenon detectors for particle physics and astrophysics," *Rev. of Mod. Phys.*, vol. 82, p. 2053, 2010.
- [15] K.-L. Giboni, E. Aprile, P. Majewski, K. Ni, and M. Yamashita, "Fast timing measurements of gamma-ray events in liquid xenon," *IEEE Trans. Nucl. Sci.*, vol. 52, p. 1800, 2005.
- [16] V. M. Atrazhev, A. V. Berezhnov, D. O. Dunikov, I. V. Chernysheva, V. V. Dmitrenko, and G. Kapralova, "Electron transport coefficients in liquid xenon," in *Proc. 2005 IEEE Int. Conf. Dielect. Liquids*, Jul. 2005, p. 329.
- [17] V. Solovov, V. Chepel, A. Pereira, M. I. Lopes, R. Ferreira Marques, and A. J. P. L. Policarpo, "Two-dimensional readout in a liquid xenon ionisation chamber," *NIMA*, vol. 477, p. 184, 2002.
- [18] E. Aprile, A. Curioni, K. L. Giboni, M. Kobayashi, U. G. Oberlack, and S. Zhang, "Compton imaging of MeV gamma-rays with the Liquid Xenon Gamma-Ray Imaging Telescope (LXeGRIT)," *NIMA*, vol. 593, p. 414, 2008.
- [19] P. Amaudruz, D. Bryman, L. Kurchaninov, P. Lub, C. Marshall, and J. P. Martin, "Simultaneous reconstruction of scintillation light and ionization charge produced by 511 keV photons in liquid xenon: Potential application to PET," *NIMA*, vol. 607, pp. 668–676, 2009.
- [20] E. Aprile, K. L. Giboni, P. Majewski, K. Ni, and M. Yamashita, "Observation of anticorrelation between scintillation and ionization for MeV gamma rays in liquid xenon," *Phys. Rev. B*, vol. 76, p. 014115, 2007.
- [21] C. Grignon, J. Barbet, M. Bardies, T. Carlier, and J. F. Chatal *et al.*, "Nuclear medical imaging using  $\beta^+\gamma$  coincidences from  $^{44}\text{Sc}$  radionuclide with liquid xenon as detection medium," *NIMA*, vol. 571, p. 142, 2007.
- [22] R. A. Holroyd, S. Geer, and F. Ptohos, "Free-ion yields for several silicon-, germanium-, and tin-containing liquids and their mixtures," *Phys. Rev. B*, vol. 43, p. 9003, 1991.
- [23] S. Geer and R. A. Holroyd, "Electron thermalisation lengths and total initial-ionisation yields in tetra-alkyls liquids," *Phys. Rev. B*, vol. 46, p. 5043, 1992.
- [24] B. Aubert, J. Colas, L. Dobrzynski, Ph. Ghez, D. Krynn, and J. C. Lacotte *et al.*, "Saturation of ionization signals in TMP and TMS at different angles and electric fields," *NIMA*, vol. 286, p. 147, 1990.
- [25] R. A. Holroyd and E. Norton, "Radiation chemistry of tetramethylgermane," *Radiat. Phys. Chem.*, vol. 39, p. 345, 1992.
- [26] P. Salin, "La calorimétrie à liquide organique diélectrique a température ambiante: étude des propriétés dans la perspective du LHC," PhD Thesis, Paris VI University, Jul. 6, 1993.
- [27] C. Silvestru, H. J. Breunig, and H. Althaus, "Structural chemistry of bismuth compounds. I. Organobismuth derivatives," *Chem. Rev.*, vol. 99, pp. 3277–3327, 1999.
- [28] L. D. Freedman and G. O. Doak, "Preparation, reactions, and physical properties of organobismuth compounds," *Chem. Rev.*, vol. 82, pp. 15–57, 1982.
- [29] O. Bunemann and T. E. Cranshaw, "Design of grid ionisation chambers," N. R. C. of Canada vol. 1986, 1949, p. 191.
- [30] O. Gevin, F. Lugiez, E. Delagnes, O. Limousin, and A. Meuris, "IDeF-X SX0: A Low Power CMOS ASIC for the readout of Cd(Zn)Te Detectors," in *Proc. IEEE-NSS Conf. Rec.*, 2009, p. 318.
- [31] O. Gevin, P. Baron, X. Coppolani, F. Daly, E. Delagnes, and O. Limousin *et al.*, "IDeF-X ECLAIRs: A CMOS ASIC for the Readout of CdTe and CdZnTe Detectors for High Resolution Spectroscopy," *IEEE Trans. Nucl. Sci.*, vol. 56, p. 2351, 2009.
- [32] O. Limousin, F. Lugiez, O. Gevin, A. Meuris, C. Blondel, and E. Delagnes *et al.*, "Caliste 256: A CdTe imaging spectrometer for space science with a 580  $\mu\text{m}$  pixel pitch," *NIMA*, vol. 647, pp. 46–54, 2011.

- [33] W. F. Schmidt, G. Bakale, A. Khrapak, and K. Yoshino, "Drift velocity of ions and electrons in non-polar dielectric liquids at high electric field strengths," in *Proc. IEEE Int. Conf. Dielect. Liq.*, Jun. 2011, pp. 1–4.
- [34] H. Hara, H. Ohnuma, Y. Hoshi, H. Yuta, K. Abe, and F. Suekane *et al.*, "A study of energy resolution in a gridded ionisation chamber filled with tetramethylsilane et tetramethylgermanium," *Rad. Meas.*, vol. 29, pp. 1–8, 1998.
- [35] P. Verrecchia, E. Ramos, D. Yvon, G. Tauzin, and V. Reithinger, "CaLIPSO: TMBi properties for particles detection," in *Proc. IEEE TNS-MIC Conf. Rec.*, Anaheim, CA, 2012, in press.
- [36] P. H. Tewari and G. R. Freeman, "Dependence of radiation-induced conductance of liquid hydrocarbons on molecular structure," *J. Chem. Phys.*, vol. 49, p. 4394, 1968.
- [37] W. F. Schmidt and A. O. Allen, "Mobility of electrons in dielectric liquids," *J. Chem. Phys.*, vol. 50, p. 5037, 1969.
- [38] B. Johansson and G. Wickman, "General collection efficiency for liquid isoctane and tetramethylsilane used as sensitive media in parallel-plate ionization chamber," *Phys. Med. Biol.*, vol. 42, p. 133, 1997.
- [39] J. Pardo, L. Franco, F. Gomez, A. Iglesias, R. Lobato, and J. Mosquera *et al.*, "Free ion yield observed in liquid isoctane irradiated by gamma rays. Comparison with Onsager theory," *Phys. Med. Biol.*, vol. 49, p. 1905, 2004.
- [40] B. Aubert, A. Bazan, B. Beaugiraud, J. Colas, T. Leflour, and M. Maire *et al.*, "A search for materials compatible with warm liquids," *NIM A*, vol. 316, pp. 165–173, 1992.
- [41] J.-D. Gallezot, M. A. Bottlaender, J. Delforge, H. Valette, W. Saba, and F. Dollé *et al.*, "Quantification of cerebral nicotinic acetylcholine receptors by PET using 2-[<sup>18</sup>F]fluoro-A-85380 and multiinjection approach," *J. Cerebral Blood Flow & Metabolism*, vol. 28, p. 172, 2008.
- [42] S. Kopar, R. Dolenc, P. Krizan, R. Pestotnik, and A. Stanovnik, "Study of TOF PET using Cherenkov light," *NIM*, vol. A654, p. 532, 2011.
- [43] S. Kopar, R. Dolenc, P. Krizan, R. Pestotnik, and A. Stanovnik, "Study of TOF PET using Cherenkov light," *Phys. Procedia*, vol. 37, p. 1531, 2012.